Journal of Applied Polymer Science

Ternary Elastomer Nanocomposites Based on NR/BR/SBR: Effect of Nanoclay Composition

M. Zarei,[1] G. Naderi,[2]* G. R. Bakhshandeh,[2] S. Shokoohi[3]

[1]Graduate studies department, Polymer Engineering Department, Islamic Azad University, South Tehran branch, Tehran, Iran

[2]Department of Rubber, Iran Polymer and Petrochemical Institute, Tehran, Iran

[3]Polymer Engineering Department, Amirkabir University of Technology, Tehran, Iran

Correspondence to: G. Naderi (E-mail: g.naderi@ippi.ac.ir)

ABSTRACT: Elastomer nanocomposites based on natural rubber (NR), butadiene rubber (BR), and styrene butadiene rubber (SBR) containing Cloisite 15A were prepared using a two-roll mill. Mechanical, morphological, and rheological characterization of the prepared nanocomposites was carried out in order to study the effect of different nanoclay compositions, i.e., 1, 3, 5, 7, and 10 wt %. Intercalation of the elastomer chains into the silicate layers was evidenced by *d*-spacing values calculated according to the results of the X-ray diffraction (XRD) patterns. This was directly confirmed by transmission and scanning electron microscopy (TEM and SEM). The results depict a decreasing trend in the optimum cure time (t_{90}) and scorch time (t_5) values of the nanocomposite samples with increasing nanoclay loading; where the elastic modulus (G') and complex viscosity (η^*) of the samples considerably increased. The mechanical properties of the nanocomposites show a considerable increase in the tensile modulus of NR/BR/SBR/Cloisite 15A nanocomposites. © 2012 Wiley Periodicals, Inc. J. Appl. Polym. Sci. 000: 000–000, 2012

KEYWORDS: elastomer; nanocomposite; mechanical properties

Received 3 July 2011; accepted 12 March 2012; published online
DOI: 10.1002/app.37687

INTRODUCTION

Polymer/clay nanocomposites have been the focus of extensive investigations in recent years due to their advanced potential applications even with the addition of very small weight percentages (<5 wt %) which is mainly ascribed to the nanoscale dimension of silicate layers dispersed within the polymer matrix. This causes a strong interfacial interaction between silicate layers and polymer chains, leading to a considerable progress in the thermal stability, mechanical, dynamic-mechanical, barrier, optical properties, and fire resistance compared to properties of their micro-counterparts or conventional filled polymers. In most of the polymer/clay nanocomposites reported so far, clay minerals have been widely used as reinforcing agents of choice because of their cheapness and easy availability.[1]

Blending nanoclay with polymers results in two general morphologies, intercalated in which clay is distributed in the matrix in a lamellar state and polymer chains diffuse into the galleries and exfoliated known as the complete delamination and dispersion of monolayers in the matrix.[2] The key factor to achieve optimum mechanical properties is controlling the phase morphology of nanocomposites specially distribution and dispersion of clay within the polymer matrix.

Introduction of nanomaterials attracted attentions to the synergistic properties of combining the two complementary technologies of elastomer blends and nanocomposites. Very recently, increasing attention has been paid on elastomer nanocomposites. According to reports, several rubber/clay nanocomposites (RCNs) have been prepared via solution intercalation, melt intercalation, and rubber-latex compounding.[3–6] Shan et al.[7] believe that the reduction of scorch and cure times of natural rubber (NR)/styrene butadiene rubber (SBR) nanocomposites indicated the accelerating effect of alkyl ammonium salts present in the organoclay molecular structure on the vulcanization process compared to carbon black counterparts. This behavior has been reported in similar research studies.[8,9] Rahmatpour et al.[10] reported that the tensile strength, elongation at break, and hardness (shore A) increased with increasing clay content up to 6 phr in solution intercalated NR/SBR nanocomposites and then remained almost constant. Song and Wong[11] studied the effect of two different types of nanoclay on the mechanical properties of butadiene rubber (BR) and SBR nanocomposites. They observed a 10-fold increase in the tensile strength of SBR/

Table I. Composition (wt %) and Nomenclature of the Nanocomposite Samples Prepared

Sample code	NR	BR	SBR	e 15A Cloisit
NBS0	65	20	15	0
NBS1	65	20	15	1
NBS3	65	20	15	3
NBS5	65	20	15	5
NBS7	65	20	15	7
NBS10	65	20	15	10

Clay nanocomposites compared to the SBR gum. Zhang and Wang[12] mentioned that stronger adhesion between the elastomer chains and clay galleries would result in finer dispersions and consequently higher mechanical properties. A study on NR/BR nanocomposites showed that no diffraction peaks is observed in XRD patterns of the nanocomposites samples before vulcanization process; where the relative characteristic peak in the vulcanized nanocomposites is reprehensive of intercalated microstructure.[8]

Regarding the abovementioned, there exist some research studies on the elastomer nanocomposites based on one or two elastomers containing different types of nanoclay; to the best of our knowledge, no studies have been published on (NR/BR/SBR) nanocomposites in the literature. In this article, effect of nanoclay composition on different properties of these nanocomposites has been investigated.

EXPERIMENTAL

Material

Natural rubber (SMR20: Mooney viscosity ML(1+4)100°C = 55 M; density = 0.913 g/cm^3), BR (BR1220; Mooney viscosity ML(1+4)100°C = 45 M; density = 1.02 g/cm^3), and SBR (SBR1502: Mooney viscosity ML(1+4) 100°C = 52 M; density = 0.94 g/cm^3) were, respectively, supplied by Malaysia Rubber Co., Arak Petrochemical complex, and Bandar Imam Petrochemical complexes. The curing system including CZ ($C_{13}H_{16}N_2S_2$) and D ($C_6H_5NHC(=NH)NHC_6H_5$) accelerators, zinc oxide activators, stearic acid, and sulfur used here were produced by Lanxess, Rangine Pars, Penany, China, Tianjin jixin Co., respectively. The nanoclay used was Cloisite 15A (density = 1.66 g/cm^3) which was a natural montmorillonite modified with a dimethyl dehydrogenated tallow quaternary ammonium having a cation exchange capacity of 125 mequiv/100 g.

Preparation

Nanocomposite samples, after a 2 min milling mastication of NR and pre-drying of clay at 80°C for 24 h, were prepared by a 2 kg Polymix 200 L two-roll mill for 15 min at 30°C, according to the compositions summarized in Table I. It should be mentioned that, NR, BR, SBR, zinc oxide, and stearic acid were premixed and then, the clay powder and curing agents were added to the compound in a final stage. Curing process was carried out under a Dieffenbacher hot press at 175°C and 150 bar.

Characterization

Tensile strength and elongation at break of the compression molded samples were carried out according to ASTM D 412 by a Hiwa machine at a cross head speed of 500 mm/min. Zwick Rheometer (ASTM D2084), Zwick abrasion tester (ASTM D5963), Frank Durometer (ASTM D2240), Monsanto (ASTM D2284), Doli (ASTM D623), and Frank (ASTM D1054) were used to study the cure characteristics, hardness, fatigue, heat build-up, and resilience of compounds, respectively. To evaluate compression set, compounds were placed between two standard parallel plates for a specific duration at 70°C.

The rheological measurements were performed using Alpha Technology oscillatory rheometer (RPA2000) at 80°C with parallel plate geometry (plate diameter of 25 mm, gap of 3 mm).

To evaluate the dispersion of the clay in the polymer matrix, X-ray diffraction (XRD) was performed at room temperature using an X-ray diffractomer (Philips model X'Pert) in the low angle of 2θ. The X-ray beam was a Cu Kα radiation (λ = 1.540598 Å) using a 50 kV voltage generator and a 40 mA current. XRD samples of a 2 mm thickness were prepared by a hydraulic press. The basal spacing of silicates was estimated from the position of the plane peak in the XRD intensity profile using the Bragg's law, $d = \lambda/(2\sin\theta_{max})$. The nanostructure of the nanocomposites was observed by a Tescan scanning electron microscope (SEM) and also transmission electron microscopy (TEM) (Philips EM-2085) of cryogenically microtomed (with a diamond knife at −100°C) fracture surface of the samples with a voltage accelerator of 100 kV.

Gel content values were calculated according to the weight loss of the sample washed with acetone after a 24 h dipping in boiling toluene.

Dynamic mechanical analysis (DMA) was performed using a Tritec 2000 DMA system (Triton Technology, UK). Storage modulus and damping characteristics of the samples were determined as a function of temperature. Temperature scan was done from −100°C to +100°C at a frequency of 1 Hz. The heating rate used was of 5 °C/min.

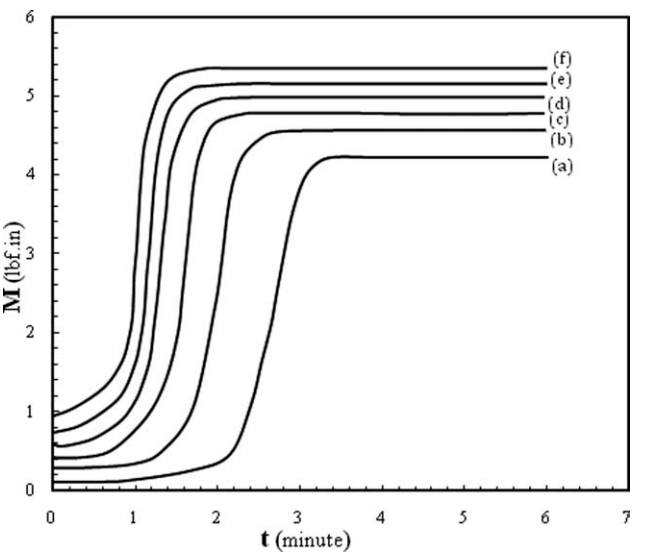

Figure 1. Cure curves of NR/BR/SBR (65/20/15) nanocomposites containing (a) 0, (b) 1, (c) 3, (d) 5, (e) 7, and (f) 10 wt % Cloisite 15A.

Table II. Cure Characteristics Measured for NR/BR/SBR/Organoclay Nanocomposites

Sample code	t_5 (min)	t_{90} (min)	Rate of cure (%/min)	$M_H - M_L$ (lbf.in)
NBS0	2.11	3.1	88.2	36.34
NBS1	1.34	2.1	98.1	38.00
NBS3	1.11	1.9	110.6	38.84
NBS5	0.98	1.8	117.2	40.70
NBS7	0.77	1.6	120.4	41.80
NBS10	0.65	1.5	123.1	42.91

RESULTS AND DISCUSSION

Cure Characteristics

Figure 1 compares the cure curves of NR/BR/SBR (65/20/15) elastomer blend and nanocomposite samples based on these compounds containing 1, 3, 5, 7, and 10 wt % organoclay. As expected,[13–15] optimum cure time (t_{90}) and scorch time (t_5) of the samples are decreased, increasing the clay content. This would consequently increase the cure rate and torque values ($\Delta M = M_H - M_L$) of prepared compounds. Thus, the organoclay is not only a reinforcing agent but also behaves as an effective accelerant or co-curing agent for vulcanization process of NR/BR/SBR. Vulcanization process is generally intensified at higher pH values.[9] In fact, functional amine groups of organic cations extracted from the organoclay gallery spacing form coordination complexes[3,4,16] facilitating the development of elemental sulfur[17,18] and curing reaction of NR, BR, and SBR stocks.[19,20] Possible formation of Zn complexes in which sulfur and ammonium functional modifying groups participate may facilitate the formation of crosslinks. Therefore, introduction of small amount of organoclay to NR/BR/SBR elastomer blends, conventionally used in tire industry, would reduce the vulcanization process duration.

The cure curves depicted in Figure 1 show that the torque data ($\Delta M = M_H - M_L$) rise with the clay loading, as expected (see Table II). It is believed that, the smaller the particle size is, the larger the surface area will be. This would lead to greater rubber–filler interactions imposing extra resistance to flow as a higher restriction to molecular motion of the macromolecules[21] which consequently results in an increase in the torque value.[13,14] On the other hand, the higher crosslink density of the compounds containing clay particles will consequently lead to higher torque values.[22] In fact, $M_H - M_L$ is a measure of the shear dynamic modulus, which indirectly relates to the crosslink density of the nanocomposites.[23] It can be observed in Figure 1 that with increasing the nanoclay content, torque values rise. Although this would raise the energy consumption required for the compounding process, but it would be neglected regarding the small contents of clay added to the blends and also the advantages presented by this method.

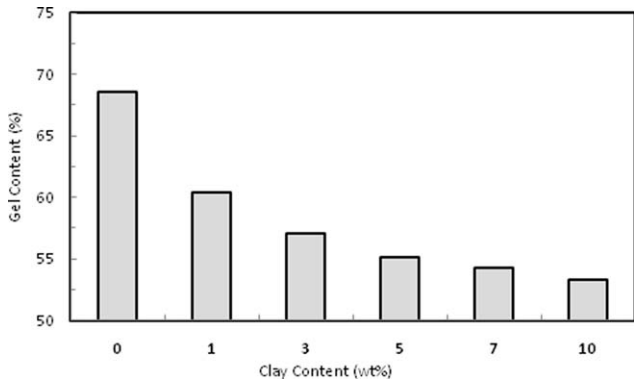

Figure 2. Gel content values of NR/BR/SBR (65/20/15) nanocomposite samples containing 0, 1, 3, 5, 7, and 10 wt % nanoclay.

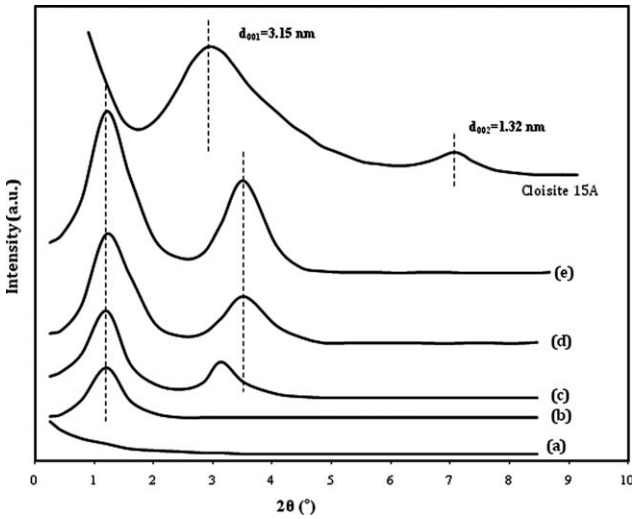

Figure 3. XRD patterns of NR/BR/SBR (65/20/15) nanocomposites containing (a) 0, (b) 1, (c) 3, (d) 5, (e) 7, and (f) 10 wt % organoclay.

Figure 2 illustrates the gel content variation of NR/BR/SBR (65/20/15) nanocomposite samples containing 0, 1, 3, 5, 7, and 10 wt % nanoclay which support the abovementioned results. As expected, addition of nanoclay particles results in an increase in the crosslink density of the samples and consequently a decrease in the gel content values.

XRD Results

XRD patterns of nanocomposite samples based on NR/BR/SBR containing different clay loadings are illustrated in Figure 3. As can be seen in this figure, no peaks is distinguished in the case of nanocomposites containing 1 wt % of organoclay, this may refer to the exfoliation of clay layers within the elastomer matrix. In all other cases, the characteristic peak of the 2424242424 basal reflection of organoclay is observed. The leftward shift of the peaks compared to the original clay ($2\theta = 2.9$; $d_{001} = 31.5$ Å), indicates the increase in the interlayer spacing of Cloisite 15A after compounding process up to 72.3 Å for NBS3.[4] The results show that an intercalated structure is formed and that the organoclay still retains an ordered structure after melt compounding. As expected, the intensity of XRD peaks increases with the clay contents. Nanocomposite sample containing 1 wt % Cloisite 15A has the lowest

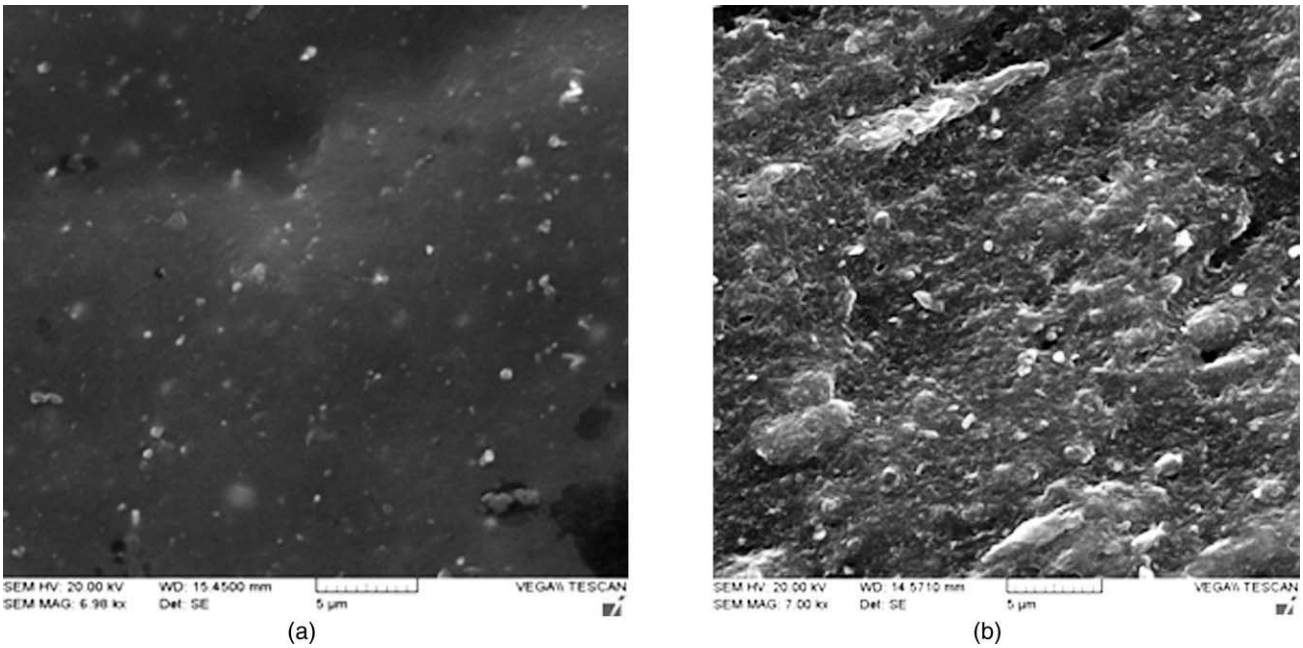

Figure 4. SEM micrographs of (a) NR/BR/SBR (65/20/15) and (b) NR/BR/SBR/Cloisite 15A (65/20/15/10) samples.

intensity among the samples with 3, 5, 7, or 10 wt % clay contents, which is ascribed to the further delamination of silicate layers.[24]

Appearance of secondary peaks in higher reflection angles observed in the patterns related to NBS5, NBS7, and NBS10 (see Figure 3) corresponds to 2424242424 plane. Rightward shift of the peak with increasing the clay content from 5 up to 10 wt % is ascribed to the packing of clay layers within the polymer matrix. This is confirmed by the TEM micrographs presented in following section.

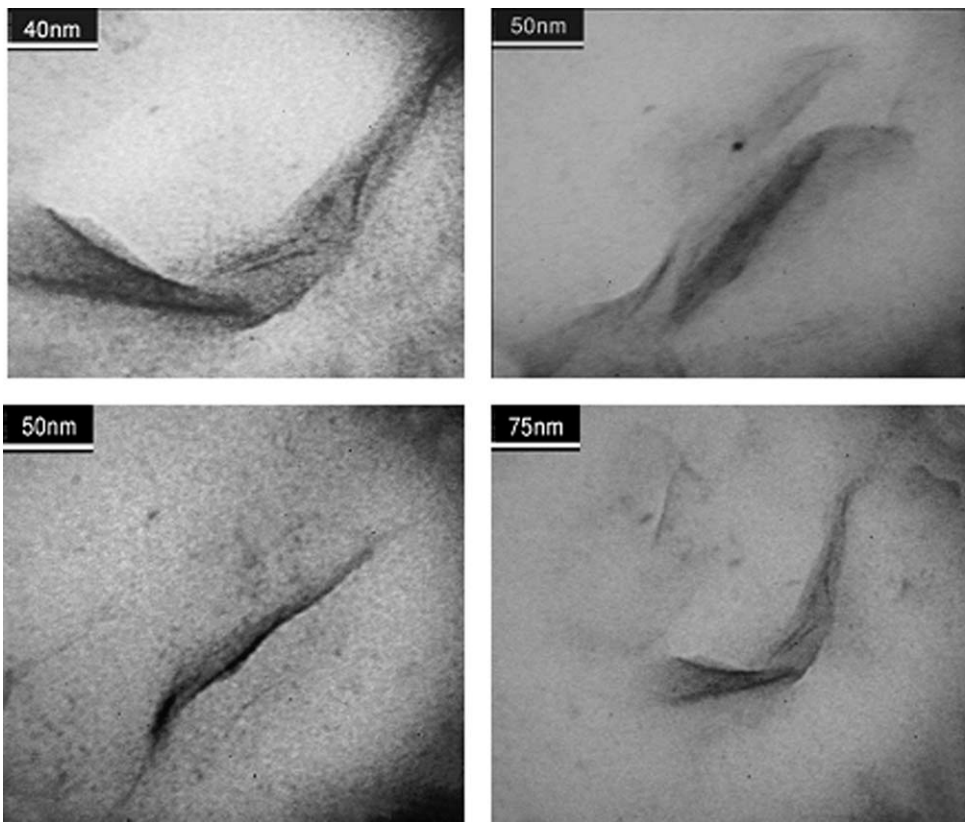

Figure 5. TEM micrographs of NR/BR/SBR/Cloisite 15A (65/20/15/5) nanocomposites with different magnifications.

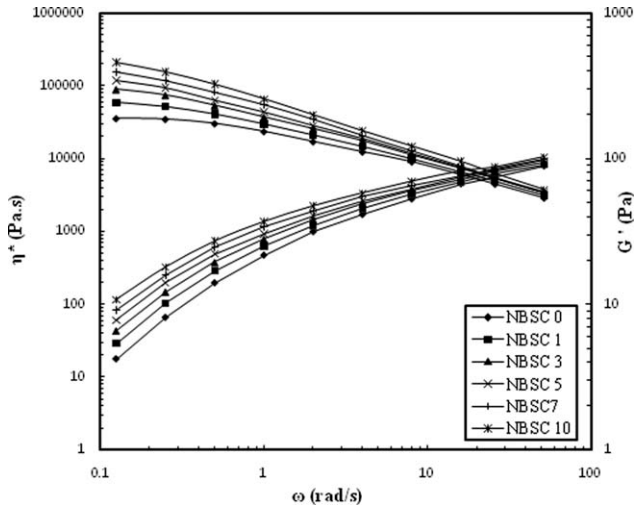

Figure 6. Complex viscosity and storage modulus of NR/BR/SBR (65/20/15) nanocomposites prepared with different nanoclay contents.

Microscopy

SEM micrographs of cryogenically fractured surface of elastomer blend sample encoded as NBS0 and also NBS10 (65NR/15BR/20SBR/10Clay) are typically presented in Figure 4. The harsh fracture surface of NBS10 [Figure 4(b)] compared to NBS0 [Figure 4(a)] is representative of good interactions between matrix and nanoparticles, implying the effective intercalation of polymer chains into the clay galleries evidenced by XRD patterns.[4]

Figure 5 shows the TEM images of cryogenically fractured surfaces of NR/BR/SBR/Cloisite 15A (65/20/15) samples containing 5 wt % of clay. Different magnifications of the micrographs confirm intercalation/partial exfoliation of the clay through the polymer matrix, evidenced by XRD patterns. Polybutadiene domains appear darker in TEM micrographs compared to the other phases (i.e., NR and SBR) due to the higher density of BR. Dark lines also represent the Cloisite layers dispersed within the matrix. Accordingly, clay seems to be mostly dispersed in BR darker phases; this phenomenon could be attributed to the lower Mooney viscosity of BR compared to NR and SBR.

Rheological Properties

Rheological measurements of NR/BR/SBR (65/20/15) nanocomposites prepared with different clay contents are illustrated in Figure 6. As expected, the complex viscosity of the nanocomposites is higher compared to the unfilled matrix, indicating the formation of a network structures and also good matrix–clay interactions resulting in a rise in the complex viscosity.[3,4,25,26] The falling trend of viscosity with frequency in Figure 6, observed in all the clay loadings, represents the pseudoplastic nature and shear thinning behavior of the compounds. The remarkable rise of complex viscosity at low frequencies could be compared to the materials exhibiting a yield stress[27] indicating that a yield stress may be present for nanocomposites compared to the pure matrix. The elastic modulus of nanocomposites also increases with clay loading which would be ascribed to the good interactions established between the matrix components and organoclay functional groups.

Mechanical Properties

As known well, abrasion resistance, fatigue life, and crack growth resistance of tire material is an essential factor to the quality of final product. Organoclays also present the potential to improve the key properties of the pure NR/BR/SBR compounds commonly used by tire industry.

Mechanical properties of the NR/BR/SBR nanocomposite samples are reported in Table III. Mechanical strength of the nanocomposites depends on different factors encompassing matrix–clay interactions, compounding conditions, microstructure, and clay content. As expected,[4,14,28] tensile strength, modulus, and hardness overall improved by increasing the clay content compared to the NBS0 elastomer blend. This improvement has been attributed to the state of intercalation/exfoliation of the nanocomposite as well as confinement of polymer chains in the presence of clay within the matrix. High *L*/*D* of silicate layers is responsible for higher resistance of polymer chains against crack growth compared to the spherical fillers used in tire industry.[28] Stress-induced orientation of clay layers under the tensile stress results in a considerable increase in the tensile properties of intercalated/exfoliated nanocomposites.[25] Physical crosslinks induced by the clay particles may also cause an improvement in the mechanical behavior of the nanocomposites. Stringently speaking, the mechanical property growth rate weakens at clay contents higher than 5 wt %. A similar trend, attributed to the filler packing and consequently formation of stress concentrator spots, has also been reported by Wang et al.,[25] Bathias and coworker[29] in NR/organoclay nanocomposites.

Table III. Mechanical Properties of NR/BR/SBR/Organoclay Nanocomposite Samples

NBS10	NBS7	NBS5	NBS3	NBS1	NBS0	Properties
11.12 ± 0.06	11.01 ± 0.04	10.89 ± 0.9	9.21 ± 0.09	8.01 ± 0.07	5.5 ± 0.08	Tensile strength (MPa)
1.70 ± 0.02	1.53 ± 0.01	1.48 ± 0.01	1.30 ± 0.02	1.08 ± 0.01	0.77 ± 0.01	Modulus (MPa)
480.41 ± 12.62	486.50 ± 11.02	490.23 ± 7.44	500.11 ± 9.23	520.70 ± 10.20	536.61 ± 6.02	Elongation at break (%)
55.71 ± 2.42	52.91 ± 1.48	50.71 ± 2.11	49.41 ± 1.67	47.72 ± 0.95	44.61 ± 1.12	Shore A hardness
18.53 ± 1.19	18.68 ± 2.21	18.98 ± 1.01	19.53 ± 1.65	19.93 ± 0.93	21.51 ± 1.41	Abrasion (wt%)
5.81 ± 0.06	6.68 ± 0.08	7.63 ± 0.09	8.51 ± 0.11	9.49 ± 0.09	10.82 ± 0.15	Compression set (%, at 70°C)
1977 ± 17	1964 ± 18	1960 ± 17	1920 ± 19	1715 ± 12	1491 ± 15	Fatigue life (Cycles)

Applied Polymer SCIENCE

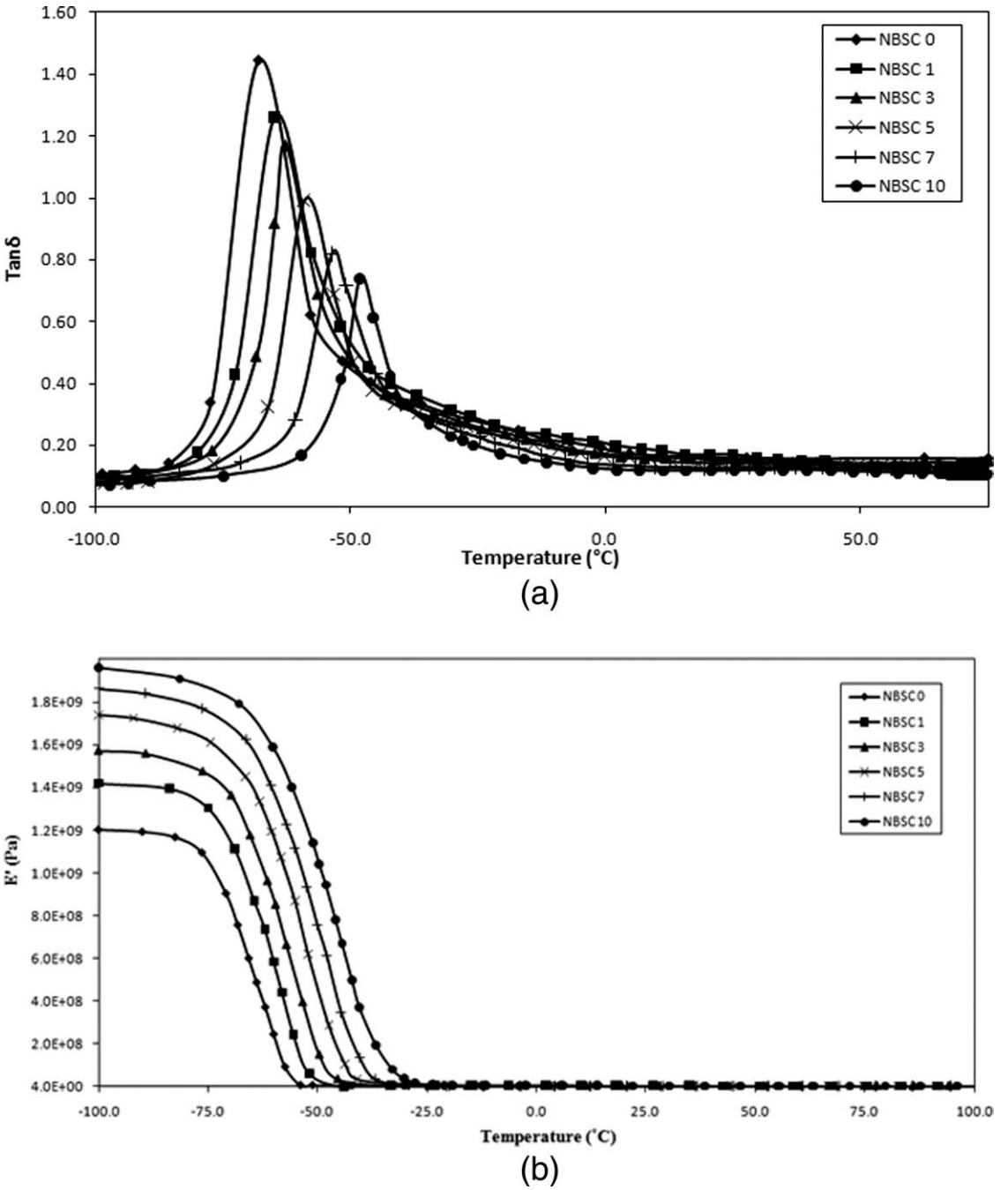

Figure 7. DMTA results for NR/BR/SBR (65/20/15) nanocomposites containing 1, 3, 5, 7, and 10 wt % Cloisite 15A.

According to Bathias and coworker,[29] increased crosslink densityin the presence of organoclay may be responsible for the decrease observed in abrasion loss and elongation at break values reported in Table III. In fact, high surface area of silicate layers results in an improvement in the clay/matrix adhesion.[11,26] This increase could be attributed to the fact that the nanoparticles supported part of the applied load, thus the penetration into the polymer surface was reduced and only microploughing and/or microcutting phenomena could be generated.

As expected, addition of clay rigid filler to NR/BR/SBR elastomer blends also increases the hardness, where resilience and compression set of the nanocomposites depicted a decreasing trend with increasing clay content. In fact, deformability of elastomer chains is restricted in the presence of clay layers.[30] Resistance to fatigue crack growth is sustained in NR/BR/SBR nanocomposites as seen in Table III like mineral-filled polymer composites.

The fatigue process has been traditionally divided into three stages: crack initiation, crack propagation, and final failure. Surface flaws and inclusions are the most common sites for fatigue crack initiation. In most engineering materials, cracks are inherently present on the surface flaws, component surface, and

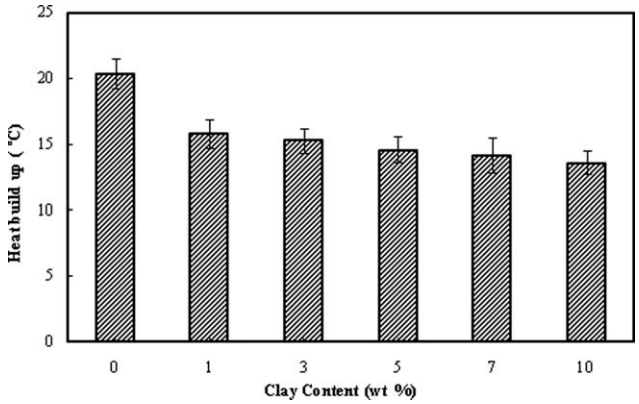

Figure 8. Heat build-up values for NR/BR/SBR (65/20/15) nanocomposites containing 1, 3, 5, 7, and 10 wt % Cloisite 15A.

second phase-matrix interface due to high local stress concentration and the discontinuity in mechanical properties at the particle–matrix interface crack initiation becomes easier. On the other hand, the lower stress concentration at the surface of nano-scaled fillers makes them less prone to cracking as compared to conventional fillers. Also, the smaller distance between two neighboring nanoparticles as the result of higher density is effective in crack bowing and pinning.[31] According to Sirvastava and Koratkar,[31] the fatigue crack might also be bridged by high aspect ratio organoclay layers generating a bridging zone in the wake of the crack tip, furthermore, the crack advances energy is dissipated by the frictional pull-out of the bridging clay layers from the matrix which slows the crack propagation and consequently increases the fatigue life of nanocomposites.

Dynamic-Mechanical Properties

Results, depicted in Figure 7, show that the glass transition temperature of the prepared compounds increases from −65.2°C for NR/BR/SBR (65/20/15) elastomer blends up to −48.1°C for the similar nanocomposites containing 10 wt % organoclay. This is attributed to the restriction of elastomer chains in the presence of clay layers. It should also be mentioned that the upward shift observed in the curves with increasing clay loading is the result of high aspect ratio and interactions of the nanofiller with the polymer matrix.

Traction properties of automotive tires on both dry and wet surfaces are a measure of the vehicle security. Accordingly, rubbers with high energy loss such as SBR are utilized as the tread material components. However, keeping the balance between tire rolling and wet skid resistance has been a challenge, as improving one would sacrifice the other.[32] Saito's[34] work corresponded tan δ values at 0°C and 60°C to wet skid resistance (WSR) and rolling resistance of rubber compounds; therefore the ideal tread material is required to depict a combination of high tan delta value at 0°C and low tan δ value at 60°C. Results show that nanocomposites samples containing 3 and 5 wt % (i.e., NBS3 and NBS5) depict a more balanced behavior (i.e., high WSR and low rolling resistance) compared to others. Therefore, as can be easily distinguished, addition of nanoclay would improve the vehicle security along with its energy saving effect.

Regarding the fact that NR/BR/SBR elastomer blends are commonly used in the tire treads, heat build-up characteristics of the compound would be a determining factor in the engineering material selection for this application. As can be seen in Figure 8, the reduction of peak intensity with further addition of organoclay is representative of lower hysteresis. This would, in turn, helps the effective lifetime of the tire product.

CONCLUSION

Elastomer nanocomposites based on NR/BR/SBR (65/20/15) containing different contents (1, 3, 5, 7, and 10 wt %) of Cloisite 15A were prepared using two-roll mill. Cure characterization depicted that Cloisite 15A is not only acting as a reinforcing agent but also catalyzes the curing process. In a fixed composition, gel content measurements imply an increase in the crosslink density of compounds compared to the pure NR/BR/SBR elastomer blends. XRD results showed that the organoclay still retains an ordered structure and the intercalation phenomenon has occurred. This was confirmed by TEM. Results showed a considerable improvement in mechanical properties such as tensile strength, tensile modulus, hardness, fatigue, and abrasion resistance. Furthermore, improvements observed in heat build-up and WSR ensure the positive effects of nanoclay on NR/BR/SBR (65/20/15) ternary compound as the tire tread.

REFERENCES

1. Khosrokhavar, R.; Bakhshandeh, G.; Ghoreishy, M. H. R.; Naderi, G. *J. Reinf. Plast. Compos.* **2009,** *28*, 613.
2. Sinha Ray, S.; Okamoto, M. *Polym. Sci.,* **2003,** *28*, 1539.
3. Varghese, S.; Karger-Kocsis, J. *Polymer,* **2003,** *44*, 4921.
4. Varghese, S.; Karger-Kocsis, J. *J. Appl. Polym. Sci.* **2004,** *91*, 813.
5. Urayama, K.; Kawamura, T.; Kohjiya, S. *Macromolecules,* **2001,** *34*, 8261.
6. Alipoura, A.; Naderi, G.; Bakhshandeh, G. R.; Valic, H.; Shokoohi, S. *Int. Polym. Process.,* **2011,** *2011*, 48.
7. Shan, C.; Gu, Z.; Wang, L.; Li, P.; Song, G.; Gao, Z.; Yang, X. *J. Appl. Polym. Sci.,* **2011,** *119*, 1185.
8. Kim, W.; Kim, S. *Macromol. Res.,* **2006,** *14*, 187.
9. Cataldo, F. *Macromol. Symp.,* **2007,** *247*, 67.
10. Rahmatpour, A.; Abdollahi, M.; Shojaee, M. *J. Macromol. Sci. Part B,* **2008,** *47*, 523.
11. Song, M.; Wong, C. W. *Polym. Int.* **2005,** *54*, 560.
12. Zhang, L.; Wang, Y. *J. Appl. Polym. Sci.* **2000,** *78*, 1873.
13. Lopez-Manchado, M. A.; Arroyo, M.; Herrero, B.; Biagiotti, J. *J. Appl. Polym. Sci.,* **2003,** *89*, 1.
14. Lopez-Manchado, M. A.; Herrero, B.; Arroyo, M. *Polym. Int.,* **2004,** *53*, 1766.
15. The, P. L.; Mohd Ishak, Z. A.; Hashim, A. S.; Karger-Kocsis, J.; Ishiaku, U. S. *J. Appl. Polym. Sci.,* **2004,** *94*, 2438.

16. Zheng, H.; Zhang, Y.; Peng, Z. L.; Zhang, Y. X. *Polym. Test.,* **2004,** *23*, 217.
17. Krejsa, M. R.; Koenig.J. L. The Nature of Sulfur Vulcanization in Elastomer Technology Handbook. CRC Press: Florida, **1993.**
18. Zaborski, M.; Donnet, J. B. *Macromol. Symp.,* **2003,** *194*, 87.
19. Madhusoodanan, K. N.; Varghese, S. *J. Appl. Polym. Sci.,* **2006,** *102*, 2537.
20. Mousa, A.; Karger-Kocsis, J. *Macromol. Mater. Eng.,* **2001,** *286*, 260.
21. Ismail, H.; Rosnah, N.; Rozman, H. D. *Polymer,* **1997,** *38*, 4059.
22. Sun, Y.; Luo, Y.; Demin, J. *J. Appl. Polym. Sci.*, **2007,** *107*, 2786.
23. Sengupta, A.; Konar, B. B. *J. Appl. Polym. Sci.,* **1997,** *66*, 1231.
24. Gopakumar, T. G.; Xanthos, M.; Xanthos, M. *Polym. Compos.* **2006,** *27*, 368.
25. Wang, Y.; Zhang, H.; Wu, Y.; Yang, J.; Zhang, L. *J. Appl. Polym. Sci.,* **2005,** *96*, 318.
26. Ranimol, S.; Rosamma, A.; Treesa, C.; Varghese, S.; Kuruvilla, J.; Sabu, T. *J. Appl. Polym. Sci.* **2006,** *101*, 2355.
27. Biswas, M.; Sinha Ray, S. *Polymer* **1998,** *39*, 6423.
28. Li, P.; Wang, L.; Song, G.; Yin, L.; Qi, F.; Sun, L. *J. Appl. Polym. Sci.* **2008,** *109*, 3831.
29. Legorgu-jago, L.; Bathias, C. *Int. J. Fatigue* **2002,** *24*, 85.
30. Naderi, G.; Razavi-Nouri, M.; Taghizadeh, E.; Lafleur, P. G.; Dubois, C. *Polym. Eng. Sci.* **2011,** *51*, 278.
31. Srivastava, I.; Koratkar, N. *J. Miner. Met. Mater.* **2010,** *62*, 50.
32. Nordsiek, K. H.; *Kautschuk Gummi Kunststoffe* **1985,** *38*, 178.
33. Saito, K. Y.; *Kautschuk Gummi Kunststoffe* **1986,** *39*, 30.